Electronic Supplementary Material (ESI) for Physical Chemistry Chemical Physics.

Electronic Supplementary Information

Interaction Between Butterfly-Like Prismatic Dislocation Loop Pairs and Planar Defects in Ni_3Al

Zhiwei Zhang [a,b], Qiang Fu [c], Jun Wang [a,*], Rong Yang [a], Pan Xiao [a], Fujiu Ke [d], and Chunsheng Lu [e]

[a] *State Key Laboratory of Nonlinear Mechanics (LNM), Institute of Mechanics, Chinese Academy of Sciences, Beijing 100190, China*

[b] *School of Engineering Science, University of Chinese Academy of Sciences, Beijing, 100049, China*

[c] *Aero Engine Academy of China, Beijing, 101304, China*

[d] *School of Physics, Beihang University, Beijing 100191, China*

[e] *School of Civil and Mechanical Engineering, Curtin University, Perth, WA 6845, Australia*

[*] *Corresponding author*: Jun Wang *(wangjun@lnm.imech.ac.cn)*

1. Interaction between PDL pairs and twinning boundary

During the interactive process between the first PDL pair and twin boundary, the pair oscillates up and down above the twinning boundary plane (see Fig. S1).

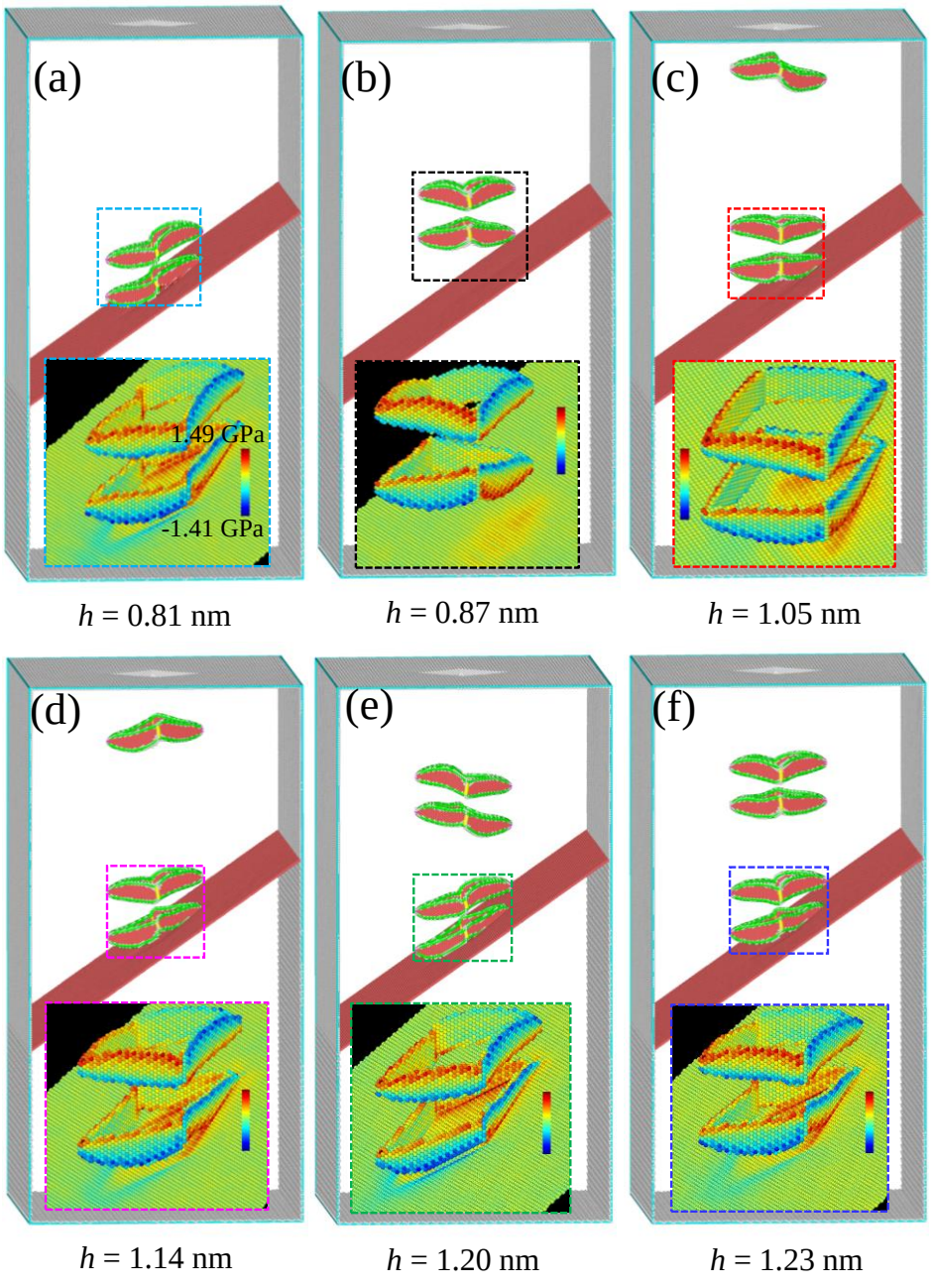

Fig. S1. Configurations analyzed by dislocation analysis in Ni_3Al with planar defect of twinning boundary at various indentation depths of (a) 0.81, (b) 0.87, (c) 1.05, (d) 1.14, (e) 1.20 and (f) 1.23 nm. Insets in (a)–(f) show stress states of the first PDL pair colored according to the shear stress τ_{yz}.

The detailed dislocation activities of interaction between PDL pairs and twinning

boundary are shown in Fig. S2. At the indentation depth of 1.35 nm, the lower wing of the first PDL pair contracts and adheres to the twinning boundary plane. At the junction region between the lower wing and twinning boundary plane, two 1/6<112> Shockley dislocations transform into two 1/6<110> stair-rod dislocations, forming two Lomer-Cottrell locks to impede the movement of this pair. This reaction also makes partial twinning boundary intersected with the lower wing migrates downward by one atomic layer (see Fig. S2a). Subsequently, the lower wing continues to shrink with the migration plane of twinning boundary gradually expanding. The two 1/6<110> stair-rod dislocations further transform into two 1/3<111> Frank dislocations while two 1/6<112> Shockley dislocations of the lower wing cross the twinning boundary plane. Meanwhile, the upper wing of the first PDL pair contacts the twinning boundary plane and reacts with the lower wing of this pair, resulting in a pinning effect (see Fig. S2b). When indentation depth increases to 1.47 nm, the lower wing of the first PDL pair gradually expands upward and approaches to the upper wing of this pair, tending to merge (see Fig. S2c). As the indentation depth continues to increase, part of the first PDL pair passes through twinning boundary, forming 1/2<110> perfect dislocations and resulting in dislocation pinning. The two wings of the first PDL pair pile up and merge on the twinning boundary plane (see Fig. S2d). After this, the second PDL pair gradually approaches the twinning boundary plane, part of the lower wing of the second PDL pair reacts with twinning boundary to produce dislocation pinning, blocking its downward movement. The other part of the lower wing of the second PDL pair reacts and merges with the first PDL pair. With indentation further increasing, more PDL pairs

continuously pile up one by one above the twinning boundary plane. It is worth noting that some of dislocations passed through the twinning boundary does not move downward any more, with the dislocation pinning state being kept (see Fig. S2e and f).

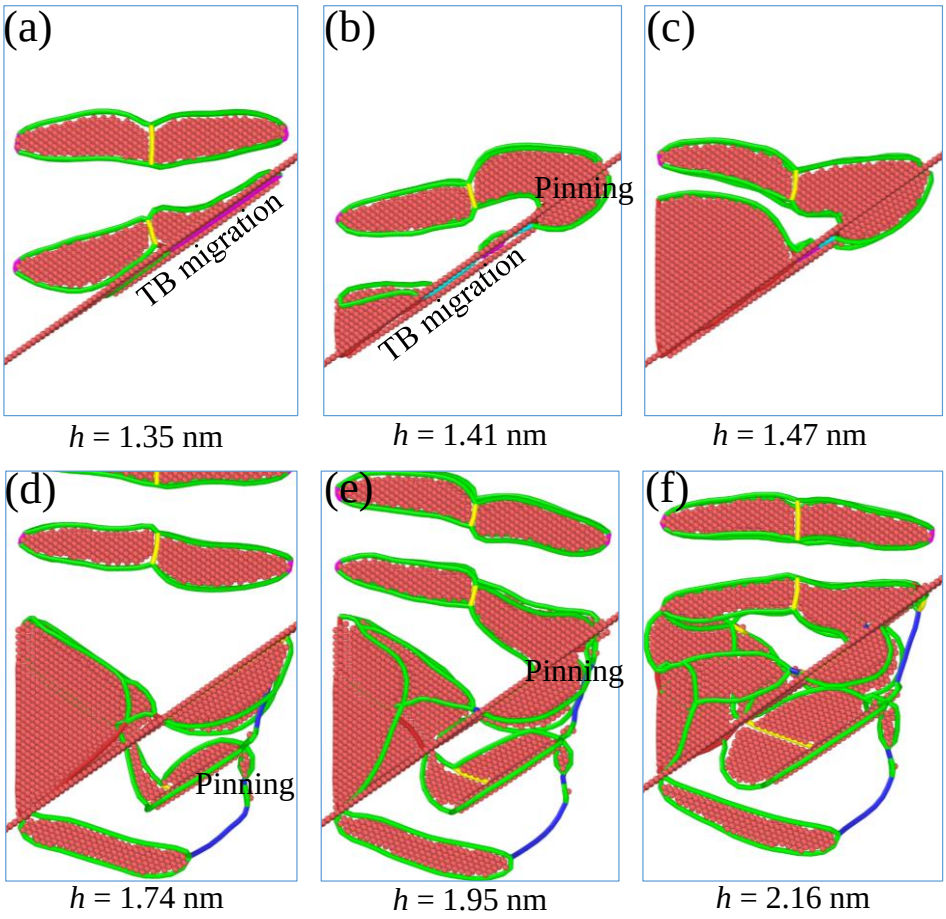

Fig. S2. Evolution of microstructures for interaction between PDL pairs and twinning boundary (TB) at various indentation depths of (a) 1.35, (b) 1.41, (c) 1.47, (d) 1.74, (e) 1.95 and (f) 2.16 nm. Atoms are colored by dislocation analysis with FCC structures removed for clarity.

2. Interaction between PDL pairs and superlattice intrinsic stacking fault

For comparison, the indentation force and interfacial potential energy of Ni_3Al with planar defect of superlattice intrinsic stacking fault are shown in Fig. S3a which can be divided into four stages. In stage I, the force curve produces two dropping points, corresponding to the activity of the first PDL pair inside the Ni_3Al matrix. As the first

PDL pair approaches the superlattice intrinsic stacking fault plane, that is, stage II in Fig. S3a, the oscillation behavior of this pair is similar to that of the first PDL pair in Ni_3Al with twinning boundary. The dynamic evolution of this PDL pair is offered in Fig. S4. At a depth of 1.17 nm (see A in Fig. S3b), the first PDL pair reaches the superlattice intrinsic stacking fault plane with its lower wing being shrunk. At this moment, the 1/6<110> stair-rod dislocation at the right half of the lower wing reacts with superlattice intrinsic stacking fault to produce dislocations pinning of several 1/6<112> Shockley dislocations on superlattice intrinsic stacking fault plane. Therefore, the lower wing of the first PDL pair lies on the superlattice intrinsic stacking fault without passing through it. As the indentation depth increases, other PDL pairs are continuously generated. As the pattern shown at B in Fig. S3b, the first PDL pair has passed through the superlattice intrinsic stacking fault plane and disappeared from the bottom of the substrate. Following this, the second PDL pair meets the superlattice intrinsic stacking fault, causing fading of partial superlattice intrinsic stacking fault intersected with this pair. Moreover, 1/6<110> stair-rod dislocations form at the boundary of junction region between the second pair and superlattice intrinsic stacking fault. Meanwhile, the third PDL pair is gradually approaching the superlattice intrinsic stacking fault plane. In general, with the increase of indentation depth, activities of PDL pairs consist of continuous nucleation from the surface of the substrate, interaction with the superlattice intrinsic stacking fault plane, and disappearance from the bottom of the substrate (see atomic pattern at C in Fig. S3b). However, as indentation depth increases to 4.53 nm, small amount of PDL pairs penetrated the superlattice intrinsic stacking

fault adhere to the lower surface of superlattice intrinsic stacking fault, resulting in the interfacial potential energy gradually increase. With increasing the amount of PDL pairs, those PDL pairs adhering to the bottom surface of superlattice intrinsic stacking fault also gradually detach and disappear from the bottom surface of the substrate (see atomic pattern at D in Fig. S3b).

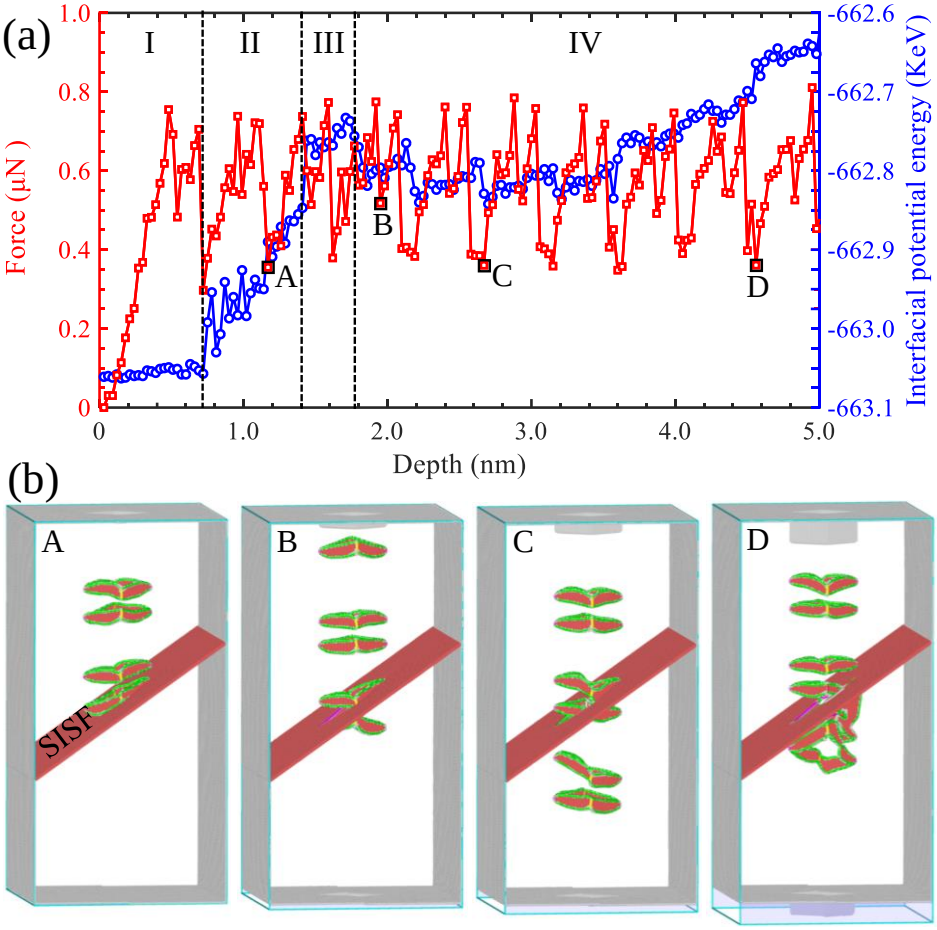

Fig. S3. Indentation force/interfacial potential energy-depth relationships of Ni_3Al with superlattice intrinsic stacking fault and corresponding atomic configurations at various indentation depths of 1.17, 1.95, 2.64 and 4.53 nm, where atoms are colored by common neighbor and dislocation analysis.

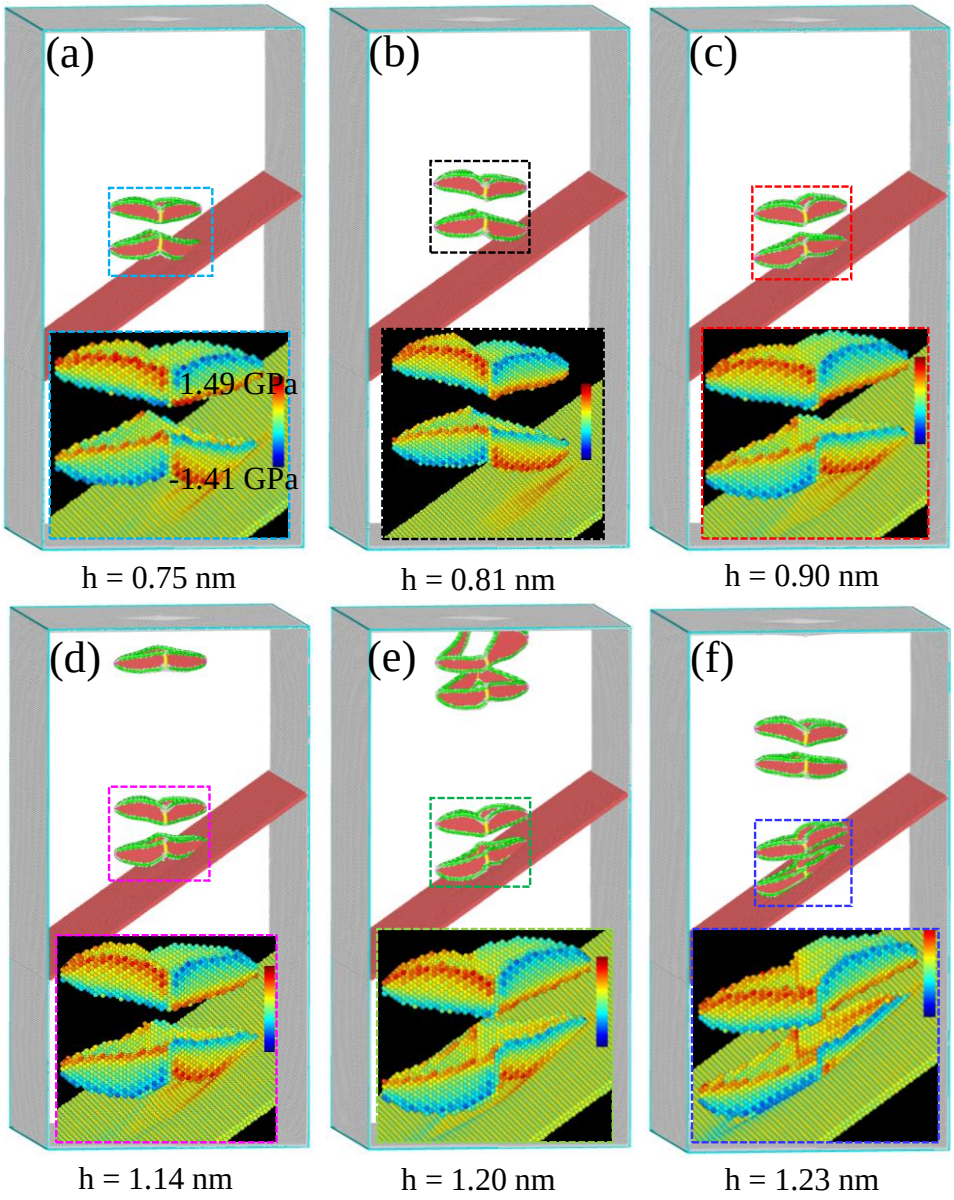

Fig. S4. Evolution of microstructures analyzed by dislocation analysis in Ni_3Al with planar defect of superlattice intrinsic stacking fault at various indentation depths of (a) 0.75, (b) 0.81, (c) 0.90, (d) 1.14, (e) 1.20 and (f) 1.23 nm. Insets in (a)–(f) show stress states of the first PDL pair colored according to the shear stress τ_{yz}.

Figure S5 shows the dislocation activities of interaction between PDL pairs and superlattice intrinsic stacking fault in stage III of Fig. S3a. When the indentation depth is 1.41 nm, the lower wing of the first PDL pair is attached to the superlattice intrinsic stacking fault plane accompanied by its own shrinkage, and the superlattice intrinsic

stacking fault remains intact (see Fig. S5a). As indentation depth reaches 1.44 nm, the right half of the lower wing of the first PDL pair passes through the superlattice intrinsic stacking fault, and this makes part of the superlattice intrinsic stacking fault fading. Meanwhile, the upper wing of this pair interacts with superlattice intrinsic stacking fault, making its two 1/6<112> Shockley dislocations and one 1/6<110> stair-rod dislocation at its right half turn into two 1/6<110> stair-rod dislocations attaching to the edge of superlattice intrinsic stacking fault faded part (see Fig. S5b). This impedes the continuous fading of superlattice intrinsic stacking fault plane. As the indentation depth further increasing, the first PDL pair continues to move downward, leading to fading of the all-region on superlattice intrinsic stacking fault intersected with the first PDL pair. The four 1/6<112> Shockley dislocations, two belonging to the left lower wing and others from the right upper wing, of the first PDL pair turn into 1/6<110> stair-rod dislocations and then attach to the faded edge area of superlattice intrinsic stacking fault (see Fig. S5c and d). When the indentation depth reaches 1.77 nm, the second PDL pair is close to the superlattice intrinsic stacking fault plane. As the indentation depth increases, the first PDL pair gradually departs from the superlattice intrinsic stacking fault, following by a mutual interaction between the second PDL pair and superlattice intrinsic stacking fault, which is similar to the reaction between the first PDL pair and superlattice intrinsic stacking fault (see Fig. S5e and f).

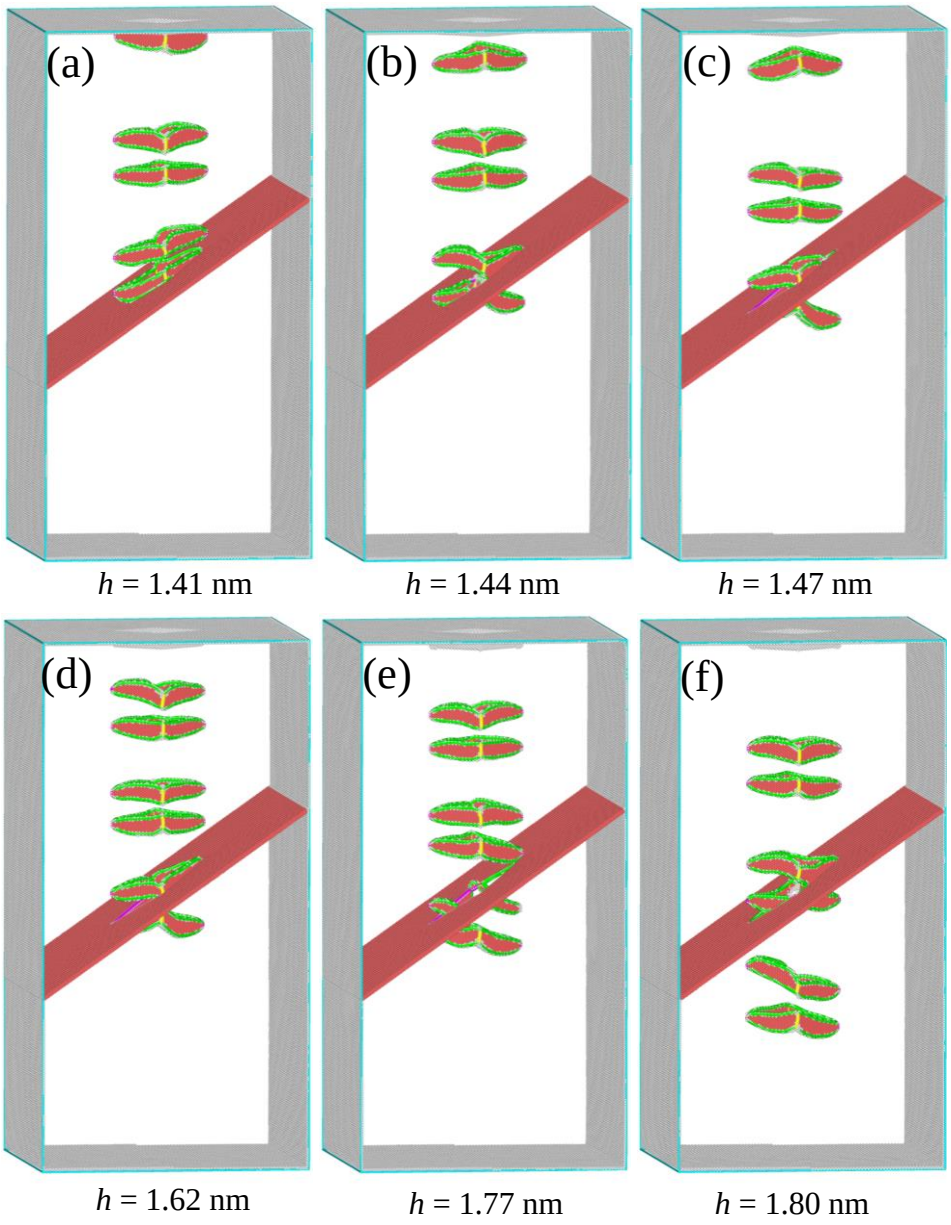

Fig. S5. Evolution of microstructures for interaction between PDL pairs and superlattice intrinsic stacking fault at various indentation depths of (a) 1.41, (b) 1.44, (c) 1.47, (d) 1.62, (e) 1.77 and (f) 1.80 nm. Atoms are colored by dislocation analysis with FCC structures removed for clarity.

3. Interaction between PDL pairs and complex stacking fault

As seen in Fig. S6a, the change trends of indentation force and interfacial potential energy of Ni_3Al with planar defect of complex stacking fault are basically the same as that of Ni_3Al with twinning boundary and superlattice intrinsic stacking fault in stage I,

in which the first PDL pair is produced during the initial indentation process. However, when the indentation depth is 0.78 nm (see A in Fig. S6b), the lower wing of the first PDL pair contacts with complex stacking fault plane, resulting in direct fading of their intersection, accompanying by generation of new 1/6<112> Shockley dislocations at the edge of faded complex stacking fault plane (see the atomic pattern at A in Fig. S6b). Meanwhile, due to the fading of partial complex stacking fault, the interfacial potential energy drastically descends. As the first PDL pair continues to move down, the complex stacking fault at the left of the PDL pair has faded and a layer of superlattice intrinsic stacking fault is generated. The newly generated superlattice intrinsic stacking fault expands along the original complex stacking fault plane before it is blocked by two 1/6<110> stair-rod dislocations as it arrives at location of the first PDL pair. The complex stacking fault on the right of the first PDL pair gradually fades with the propagation of the newly stimulated 1/6<112> Shockley dislocations on the original complex stacking fault plane (see atomic pattern at B in Fig. S6b). At this moment, the indentation force represents a rising tendency but the corresponding interfacial potential energy subjects to a sharp drop (see B in Fig. S6b). When the indentation depth is 0.84 nm, the complex stacking fault at the right side of the first PDL pair is completely replaced by the newly generated superlattice intrinsic stacking fault. Several 1/6<110> stair-rod dislocations appear at the intersection between the first PDL pair and superlattice intrinsic stacking fault (see dislocation structure at C in Fig. S6b). Thereafter, the interfacial potential energy curve also tends to be stable. Subsequently, as the indentation depth increases, the interaction mode is similar to the reaction

between PDL pairs and superlattice intrinsic stacking fault but the interfacial potential energy maintains at a stable value due to lack of adhesion of PDL pairs on bottom of the newly generated superlattice intrinsic stacking fault plane (see atomic pattern at D in Fig. S6b).

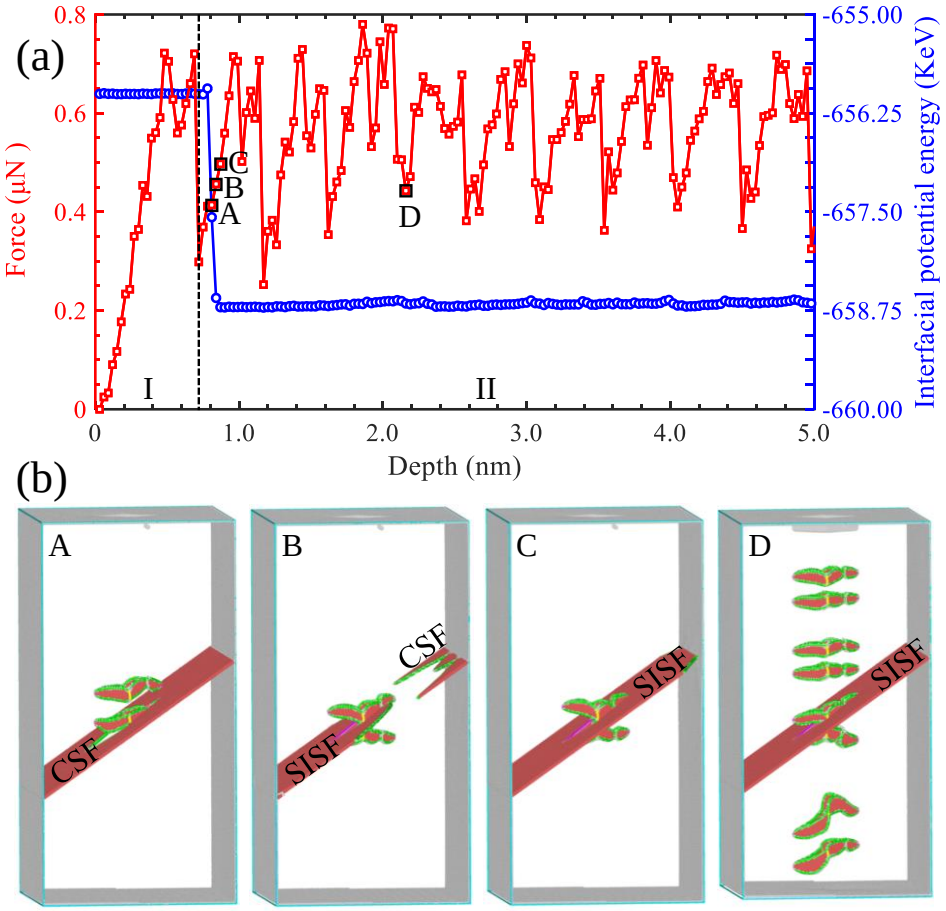

Fig. S6. Indentation force/interfacial potential energy-depth relationships of Ni_3Al with planar defect of complex stacking fault and corresponding atomic patterns at various indentation depths of 0.78, 0.81, 0.84 and 2.16 nm, where atoms are colored by common neighbor and dislocation analysis. CSF and SISF denote complex stacking fault and superlattice intrinsic stacking fault.

4. Interaction between PDL pairs and antiphase boundary

As a unique planar defect, antiphase boundary exists in Ni_3Al. The relationships between its indentation force/interface potential energy and indentation depth are

divided into three stages as shown in Fig. S7a. In stage I, indentation force and interfacial potential energy are comparable to that of substrates with other kinds of planar defects above. They all represent the nucleation and separation of the first PDL pair. However, in stage II, when the first PDL pair interacts with antiphase boundary, the interface potential energy curve shows a trend that first rises sharply, then remains stable, and finally drops suddenly, which represent a PDL pair closes to, interacts with, and separates from antiphase boundary, respectively. Moreover, the interfacial potential energy curve also shows a cyclical trend like that of the force curve.

The atomic configuration of Ni_3Al with antiphase boundary is identified according to the stress σ_z. When the indentation depth is 1.14 nm, the first PDL pair just cuts in the antiphase boundary, and the second PDL pair is initiated from the surface. This time, the interfacial region does not produce other dislocations, but part of the antiphase boundary plane intersected with the first PDL pair tends to migrate downward by an atomic layer (see pattern at A in Fig. S7b). After the first PDL pair passes through antiphase boundary, the antiphase boundary part intersected with it migrates down by two atomic layers. Then, the second PDL pair gradually approaches to antiphase boundary. Except for their shapes, the structure of PDL pairs neither changes in the process of interaction with antiphase boundary, nor does the interacting region produce extra dislocations (see pattern at B in Fig. S7b). Similarly, as the indentation depth increases, more PDL pairs move downward and pass through antiphase boundary, which cause the migration of APB intersected with them. As patterns shown at C and D in Fig. S7b, the antiphase boundary has migrated down by seven and thirteen atomic

layers, resulting from passing through of 3.5 and 6.5 PDL pairs, respectively.

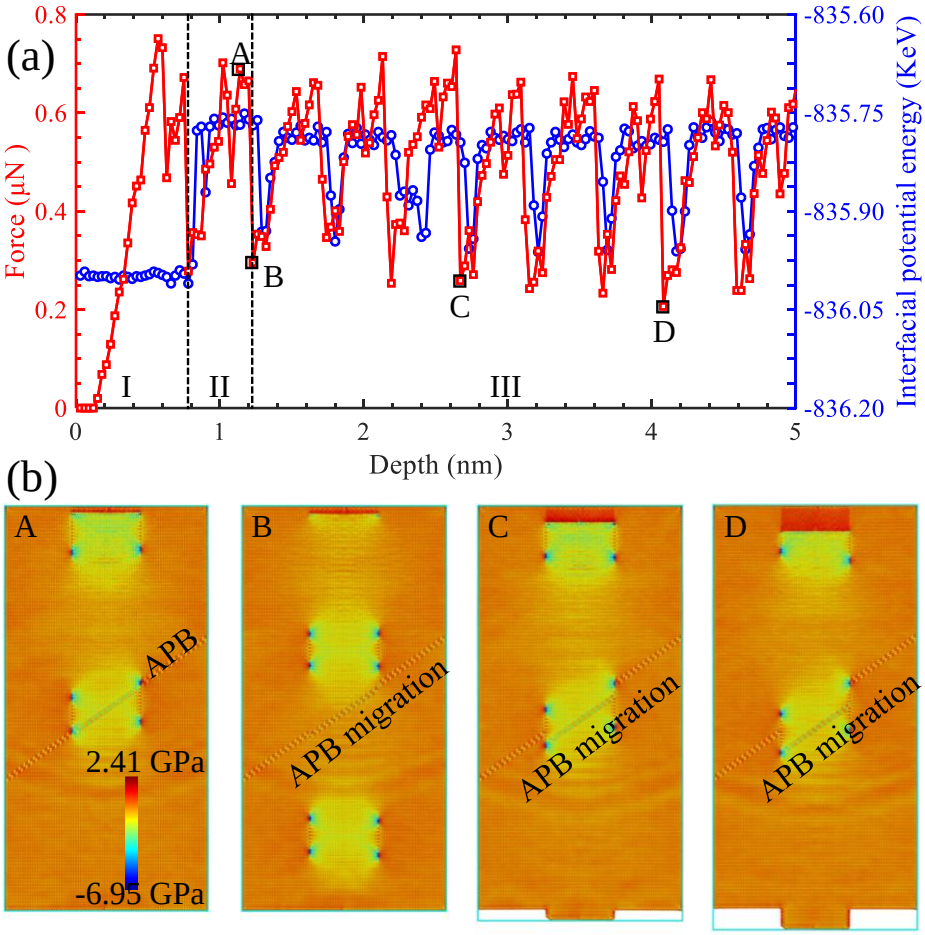

Fig. S7. Indentation force/interfacial potential energy-depth relationships of Ni_3Al with planar defect of antiphase boundary and atomic configurations at indentation depths of 1.14, 1.32, 2.61 and 3.93 nm, respectively. Atoms are colored according to the stress σ_z.

5. Collision model for hardening effect of planar defects

The relationships between indentation force/reduced hardness with various indentation depth are seen in Fig. S8.

To explain the increment of hardness resulting from planar defects, we assume that a PDL pair with the mass M and a speed v heads for an unmovable interface. After an interactive time t, its momentum loss is α ($0 \leq \alpha \leq 1$), which represents the percentage of momentum exchanged when the PDL pair collides with the interface. During this

process, the PDL pair subjects to a force

$$F_{\mathrm{PDL}} = \alpha \frac{Mv}{t} \tag{S1}$$

imposed by the interface. As the interface is continuously collided by n PDL pairs, the increment of hardness ΔH satisifies

$$\Delta H = \frac{nF_{\mathrm{PDL}}}{S}, \tag{S2}$$

where S = 4.6 ×10^{-18} m^2 is the area of indenter. Substituting Eq. (S1) into (S2), the increment of hardness can be rewritten as

$$\Delta H = \alpha \frac{nMv}{tS}. \tag{S3}$$

Since all PDL pairs lose their momentum above the twinning boundary, the corresponding value of α is 1 for all 8 collisions. On the contrary, a single crystal gets a value of 0 due to lack of any blocking mechanism. Values of α for superlattice intrinsic stacking fault and complex stacking fault are directly counted by the ratio of adhering events, 3 for both, to total collisions, 8 for both. The value of α = 0.08 for antiphase boundary is measured by variation of displacements of 9 PDL pairs after and before they cut through the antiphase boundary at a fixed time interval. In addition, the value of M = 3.07×10^{-22} kg is determined by the number of total atoms that a PDL pair contains. Value of t = 1.44×10^{-11} s is measured from the time as a PDL pair first closes to, then oscillates above and finally arrives at the interface. Value of v = 1×10^3 m s^{-1} is directly measured from motion of PDL pairs in single crystal Ni_3Al. By adopting these values, the increments of hardness resulting from twinning boundary, superlattice intrinsic stacking fault, complex stacking fault, and antiphase boundary can be derived

as 18.7, 7.1, 7.1, and 1.5 GPa, respectively, which are slightly bigger than our molecular dynamics results. This is because partial fading, transformation and migration of planar defects are not considered in the collision model.

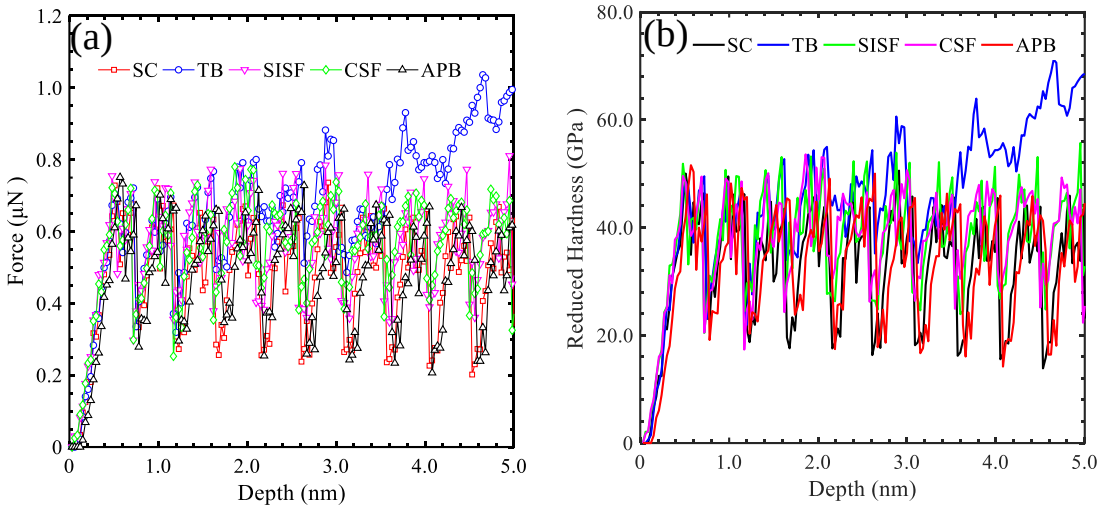

Fig. S8. (a) Indentation force and (b) hardness versus depth of nanostructured Ni_3Al.

Videos 1–5 are provided to show the dislocation activities in nanostructured Ni_3Al with single crystal, twinning boundary, superlattice intrinsic stacking fault, complex stacking fault and antiphase boundary, respectively.